Molecular dynamics simulation of pressure dependence of cluster growth in inert gas condensation

E. Kesälä, A. Kuronen, and K. Nordlund

Accelerator Laboratory, University of Helsinki, P.O. Box 43, FIN 00014 University of Helsinki, Finland
(Received 27 October 2006; published 31 May 2007)

The growth speed of nanoclusters during inert gas condensation has been studied for copper, silver, aluminum, and platinum by using molecular dynamics simulations. We determine the condensation time for vapor atoms in a particular volume to be inversely proportional to the initial partial vapor pressure. We further find that the condensation time depends on the molecular mass and lattice constant, but not on other material properties. An analytical model for the condensation time is derived from kinetic gas theory by using the basic approximations of classical nucleation theory for a homogeneous vapor.

I. INTRODUCTION

Classical nucleation theory has its roots in the study of the average behavior of particle systems, motivated largely by atmospheric science problems such as studies of aerosols, clouds, and fogs.[1–4] Study of particles, rather than particle systems, began when Bentley and Henkes in 1961 independently detected jet-generated clusters of carbon dioxide from mass spectra.[5,6] This was the starting point of the modern era of cluster science, where individual clusters can be considered as a whole system.

Nucleation of nanoparticles is important in a wide range of fields of science, for instance, in the study of organic aerosol particles in the atmosphere,[7] chemical growth of nanoparticles,[8,9] and growth of metal and semiconductor particles in gas and plasma phases for thin-film deposition.[10,11] While growth of nanoparticles by chemical means in solution and in the atmosphere has been studied extensively, less attention has been paid to growth mechanisms in inert gas environments.

In the so-called inert gas condensation nanocluster sources, free atoms of a condensed material (typically a metal or semiconductor) are first produced by, e.g., magnetron sputtering.[10,12,13] These atoms are then directed into an inert gas flow. The inert gas thermalizes the initially energetic atoms. Hence, at the initial stages of the cluster growth process, the thermalized metal or semiconductor atoms form a highly supersaturated vapor in an inert gas environment (in this paper, we will use the terms "vapor" to denote the metal atoms and "gas" to denote the inert gas ones). Inert gas condensation cluster sources are of great research and application interest, for instance, due to the possibility to grow thin films with new kinds of properties.[14–16]

The inert gas condensation differs from the atmospheric growth in some important ways: when growing semiconductors or metals, there is no nucleation barrier, and there is a high-energy release (several eV) when each new atom enters the cluster. Moreover, since the carrier gases are relatively dilute, the heating due to a new atom attachment can allow the cluster to stay hot for long times. When the nucleation barrier does not exist or is negligible, the growth models for nanoparticles cannot fully rely on equilibrium models commonly used in atmospheric and chemical sciences.

Some studies have examined the atom-level growth mechanisms of nanoclusters. It is not long ago since the efficiency of computational hardware provided sufficient means to study the gas-phase condensation of clusters in reasonable time and detail. In 1985, Thompson *et al.* applied molecular dynamics (MD) simulation method to study critical nucleus size of liquid drops in supersaturated systems containing 54 to 2048 Lennard-Jones atoms.[17] In 1997, Yasouka and Matsumoto introduced inert gas atoms to the simulated system.[18] Both of these increased the possible reactions capable of forming cluster nuclei, and gave a more natural way to treat the cooling of vapor atoms. More recently, a detailed study of inert gas condensation processes was made by Krasnochtchekov *et al.*[19,20]

In the current paper, we concentrate on the rate of cluster formation process in the level of a single nanocluster and how this rate depends on the surrounding initial vapor pressure and the element of vapor. The paper is organized as follows. We first describe the simulation method. After this, the results are presented and interpreted by an analytical model for the condensation rate. Finally, the conclusions are drawn.

II. COMPUTATIONAL METHODS

In this paper, we study the growth of Ag, Cu, Al, and Pt nanoclusters comprising of 1000 atoms by using classical MD simulations.[21] In order to realistically describe the condensation processes, we applied Berendsen thermostat[22] only to the surrounding inert gas. This method gives us more realistic heat transfer from clusters and vapor compared to any direct cooling method. In addition, the presence of argon yields more three-body collisions, which are required for nucleation to occur in a natural way. The approach has been formerly used with success in Refs. 18 and 19. The argon gas of 1000 atoms was kept at a temperature of 300 K. The use of the temperature control on the inert gas atoms only mimics the experimental situation where the inert gas remains thermal by interaction with the surroundings and being replenished from the gas flow. The initial temperature of vapor was set to 300 K.

We aimed to study the effect of initial vapor pressure to the growth speed of metal nanoclusters. The pressure was varied by changing the volume of the simulation cell while keeping other parameters, such as the number of atoms and initial temperature, fixed in different systems. This limitation

gives less freedom over possible systems to study, but at the same time, it enables modeling the effect of pressure in particular. We studied the effect by simulating the inert gas growth process at five different pressures using different metal vapors and interaction models. The simulation times depended on the initial pressure. For the highest pressures, 10 ns was sufficient, while 60 ns was needed for the lowest ones. To get reasonable statistics, ten runs were performed at each pressure with each different interaction model.

Simulations were done by using the PARCAS code.[23,24] Interactions between metal vapor atoms were modeled by the Foiles embedded atom model (EAM) potentials.[25] In addition, copper and silver vapors were also simulated using the potentials developed by Rosato, Guilope, and Legrand (RGL) [26] to assess the possible sensitivity of the results to the choice of potential. Interactions between the metal and the carrier gas argon were represented by purely repulsive potentials developed by Ziegler, Biersack, and Littmark (ZBL).[27] Forces between carrier gas atoms were modeled by the Lennard-Jones potential.[28]

Computation of the pressure from the virial theorem using the same simulation that was used for studying the cluster growth would yield erroneous values for the partial pressures in focus. Some vapor atoms nucleate almost immediately after beginning, which would cause distortion in the value. It is quite safe to assume metal vapor as ideal gas before any nucleation has started. We determined the initial partial carrier gas pressure related to a certain volume by virial calculation of a separate simulation of the same number of argon atoms with a purely repulsive potential. It is possible to determine the pressures directly from the ideal-gas theory, since we know the number of atoms, system volume, and approximate temperature of 300 K. However, calculating it from separate simulation with applied algorithm gives us more accurate picture of the collision frequency of atoms. We used five cubic simulation cells of sizes 9, 10, 12, 15, and 20 nm with corresponding pressures of 60.9, 43.6, 24.7, 12.4, and 5.21 bar, respectively.

III. RESULTS AND DISCUSSION

A. Condensation process

The condensation process can be observed to consist of three separate events that may occur simultaneously,[19] namely, nucleation, monomeric growth, and the aggregation or coagulation. At the very start, the dominating and only phenomenon is spontaneous nucleation of metal vapor. This step requires a three-body collision of two vapor atoms and a gas or vapor atom. The nucleation phase includes some more complex reactions, for example, cluster splitting which increases the amount of dimers and trimers, before small cluster nuclei appear. These events are discussed in more detail in Ref. 20. Almost immediately after formation of a few small clusters, growth occurs mainly by addition of single monomers. This rapidly decreases the number of free monomers and, of course, results in bigger clusters in the system. When monomers have mostly vanished, and clusters are large enough, growth is mainly governed by cluster aggregation. Illustration of these phases is given in Fig. 1. Depend-

ing on the system volume, the number of free monomers in the system decreased to near zero between 1 and 10 ns. Roughly half of the growth of the largest cluster took place via cluster aggregation. This increased slightly at higher pressures. Both of these characteristics can be seen in Fig. 2.

We saw very little evidence of clusters losing atoms via evaporation in our simulations. At the lowest simulated pressures, coalescence of two relatively large clusters caused separation of atoms in some cases. However, this effect was minimal. Our simulations were run at higher pressures compared to experimental values, which are typically in the range of 1–100 mbar. This means that in the simulations, clusters cool down more rapidly, while the faster growing rate induces more heat.

B. Cluster growth of different materials

We approached the growth rate of clusters by measuring the time τ_s at which a percentage s of vapor atoms in our simulation condensed into a single cluster. This condensation time varied between different pressures and materials, and, as such, gave us a method for modeling the advancement of cluster sizes versus initial vapor pressure. The observed behavior is linked to the evolution of average cluster size in macroscopic systems. While in nearly all cases the end result of the simulation was only a single cluster with no free atoms, it was essential to measure the time for some proportion of atoms to get statistically meaningful results for our purposes. Waiting for the last monomer collision would evaluate the chaotic behavior of a single wandering free particle rather than cluster growth. The cutoff used was 95% with the corresponding condensation time τ_{95}.

The temperature of metal atoms during simulations relies on two independent factors, the cooling rate and transformation of bonding energy to thermal energy. The cooling rate of vapor atoms was not controlled directly. Reference 29 suggests that the cooling rate of vapor in a rare gas relies on the mass difference between inert gas and vapor atoms. The other active parameter in our simulations was the surrounding inert gas pressure, which was equal to the initial vapor pressure. Classical energy and momentum conservation leads to most efficient energy transfer in collision between atoms of equal masses. In addition, lower mass yields more collisions at a given pressure. Figure 3 shows the behavior we observed in our simulations. The effect of the inert gas pressure on the cooling rate of the copper vapor is as expected. This effect was similar with other materials.

The temperature during the simulations varied widely between different materials. There was no significant difference in the thermal behavior between the RGL and EAM potential models, so RGL results are not included in Fig. 3. This is reasonable, since we can consider the transfer of thermal energy in our systems as a classical momentum transfer in elastic collision, and in that case, the interaction model is not essential. Platinum has the largest mass in our studies. This leads to both slower condensation and cooling, which can be seen in its low maximum temperature and a gentle descent of the curve. In the case of relatively high mass silver, we can observe similar behavior. The cohesive energy of silver is
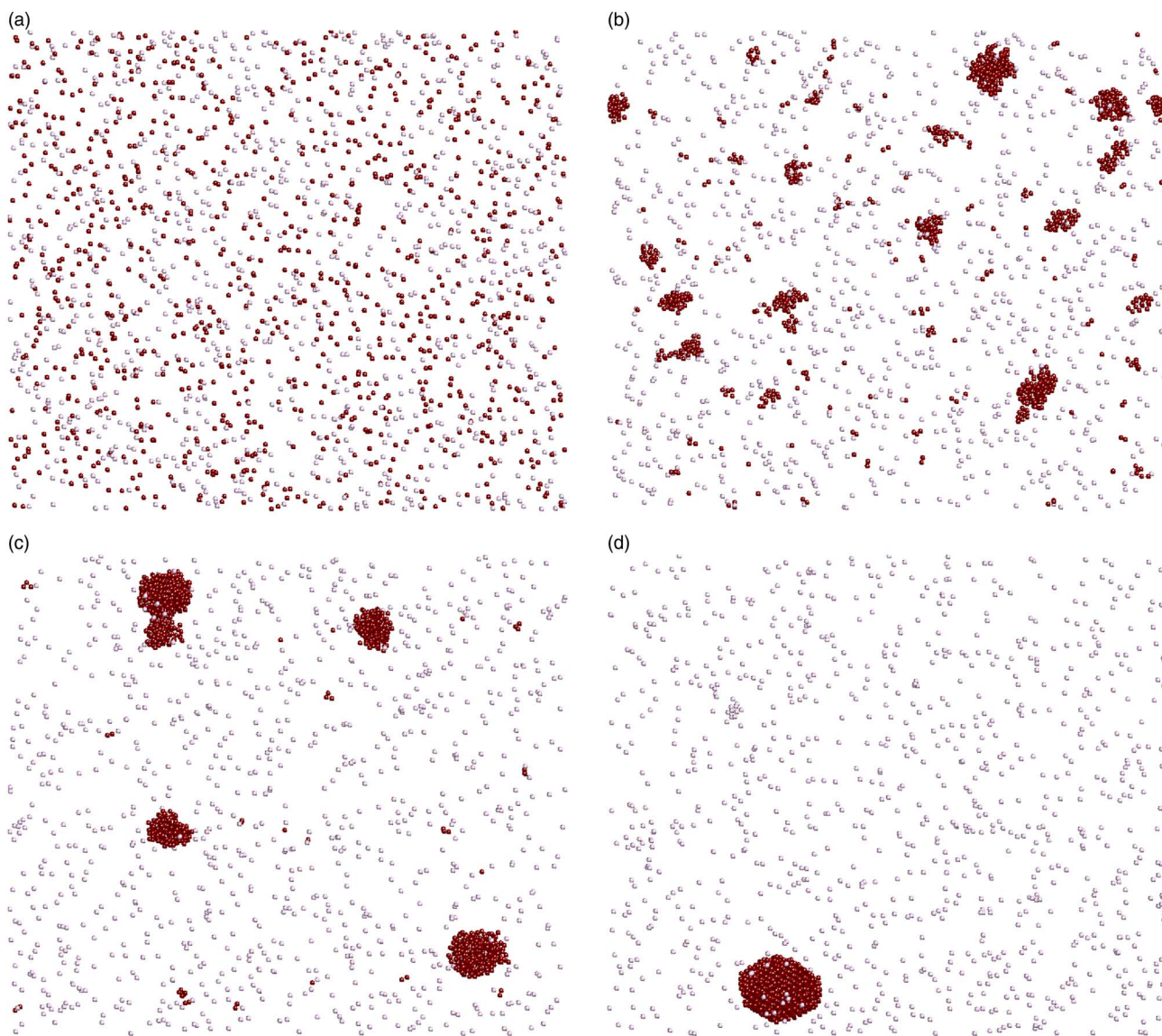
FIG. 1. (Color online) Snapshots of different phases in a typical inert gas condensation system from a single simulation in 5.21 bar pressure. Copper atoms are colored dark red and argon atoms light gray. (a) Initial state where only nucleation can occur; (b) phase of mostly monomeric growth; (c) only a few monomers left in the system, and aggregation governs growth; and (d) all copper atoms in one cluster.

significantly lower than that of platinum, which causes a lower cluster temperature even when the condensation is still faster. Copper and aluminum are closer to argon in mass, so the collisions with argon atoms exchange momentum more efficiently. In addition, the collision frequency is higher than with platinum and silver. Hence, the cooling rates [slope of $T(t)$ data in Fig. 3(b)] of Cu and Al are the highest.

Results for τ_{95} versus initial vapor pressure are presented in Fig. 4. Values for τ_{95} appeared to obey the form

$$\tau_{95} = \frac{C_c}{p_v}, \qquad (1)$$

where p_v is the initial vapor pressure and C_c a constant. In addition to the values for condensation time, Eq. (1) is fitted to the solid line in Fig. 4. Values obtained for the constant C_c by fitting are given in Table I. The similarities between values obtained for copper and silver can be explained analytically, as we will show later. There is also very little variance between values obtained with different interaction models. While in both cases simulations with the RGL potential gave a slightly smaller value for the constant C_c, the difference is almost negligible considering the statistical uncertainties of this study. This indicates that the process is not sensitive to the potential model used. A more detailed explanation for Eq. (1) and constant C_c is given in Sec. III C.

Aluminum differs significantly from copper and silver in terms of mass. At a given temperature, light aluminum atoms have larger velocities compared to copper and silver. In addition, aluminum has a relatively large lattice constant, which results in a larger volume of clusters. These characteristics increase the collision frequency of atoms and intermediate clusters, leading to a faster growth rate. Platinum, on the other hand, is substantially heavier compared to other
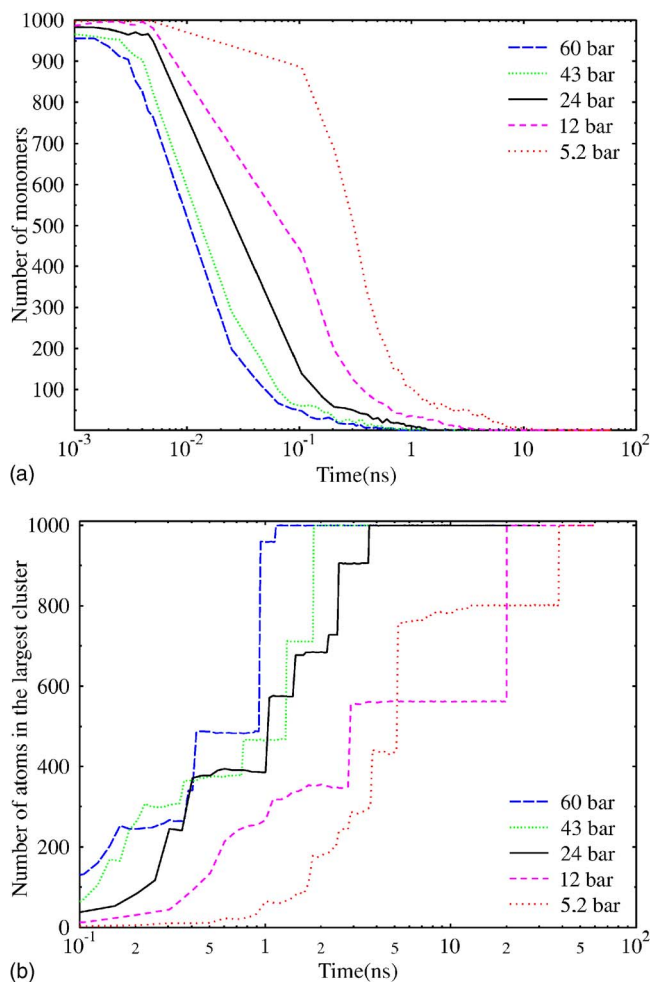
FIG. 2. (Color online) (a) Number of monomers in the system and (b) number of atoms in the largest cluster from typical condensation simulations of 1000 copper atoms in different initial pressures. Leaps in the largest clusters size indicate cluster aggregation events.

materials. While a platinum cluster of the same number of atoms has a larger volume compared to copper, its mere mass leads to a slower growth rate. Plots for aluminum and platinum are shown in Fig. 4.

C. Analytical model for condensation rate

In this section, we aim to explain the behavior observed for the growth rate of clusters in our simulations and to construct an analytical model to predict the time evolution of cluster sizes. In atmospheric physics, the evolution of cluster size distribution is mostly seen as a phase change in thermodynamic equilibrium.[30,31] In the case of inert gas condensation method, the nucleation barrier and saturation vapor pressure are negligible at the studied temperatures and time scales. The following derivation is based on assumption that the process is mainly kinetic by nature.

Formation of cluster seeds, which allows clusters to grow via addition of single monomers, occurred nearly immediately (within 5–100 ps) in our simulations. In this approach, we assume that the growth speed is dictated by the rate of
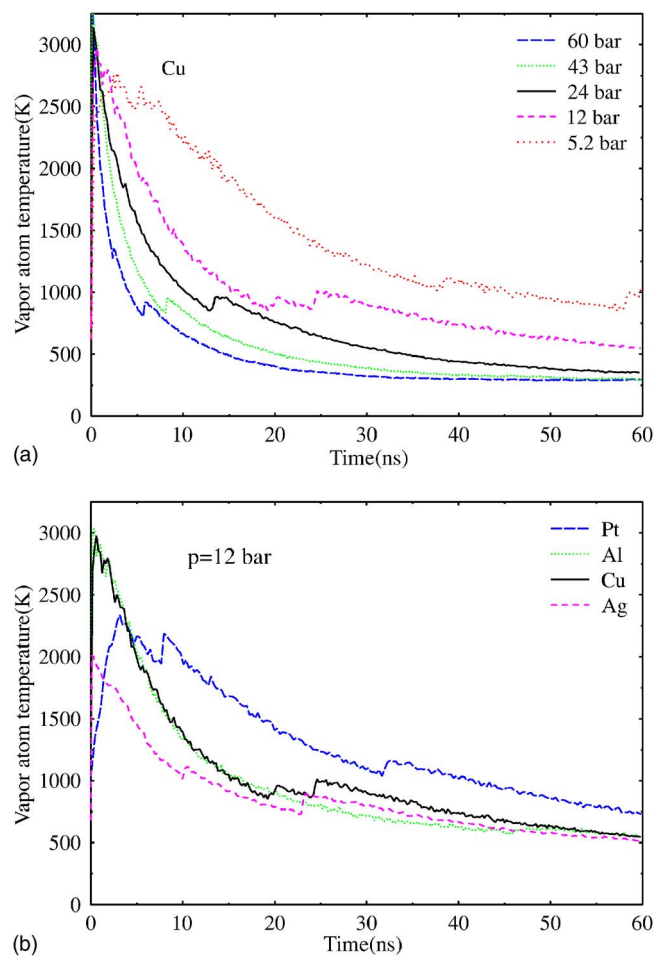
FIG. 3. (Color online) Time behavior of metal vapor temperature in the simulated systems. (a) The temperature of copper atoms at different pressures. At lower carrier gas pressures, the copper vapor cools down slower, while at the start, higher vapor pressure results in higher vapor temperature. (b) The temperature of Pt, Al, Cu, and Ag atoms at the pressure of 12 bar. Various phenomena define the temperature in different vapors. Condensation rate, bonding energy, and mass are significantly different for each material. Peaks in temperature curve result from cluster collisions, and at the end, cluster crystallization.

monomer addition. This may seem a rather crude approximation considering the snapshots of the condensation process in Fig. 1. However, at this size scale, small clusters are thermodynamically mobile in the same way as free atoms. Kinetic gas theory combined with average atom velocity in a gas yields the equation

$$z = \frac{p_v}{\sqrt{2\pi m_v k T_v}}, \qquad (2)$$

where z is the collision frequency per unit area, m_v the mass of vapor atoms, T_v the vapor temperature, k Boltzmann's constant, and p_v the initial vapor partial pressure.[31] In contrast to many situations in atmospheric science, the partial vapor pressure decreases rapidly during the growth process in simulated systems. If we include the ratio of collisions which leads to aggregation of a monomer, the so-called con-
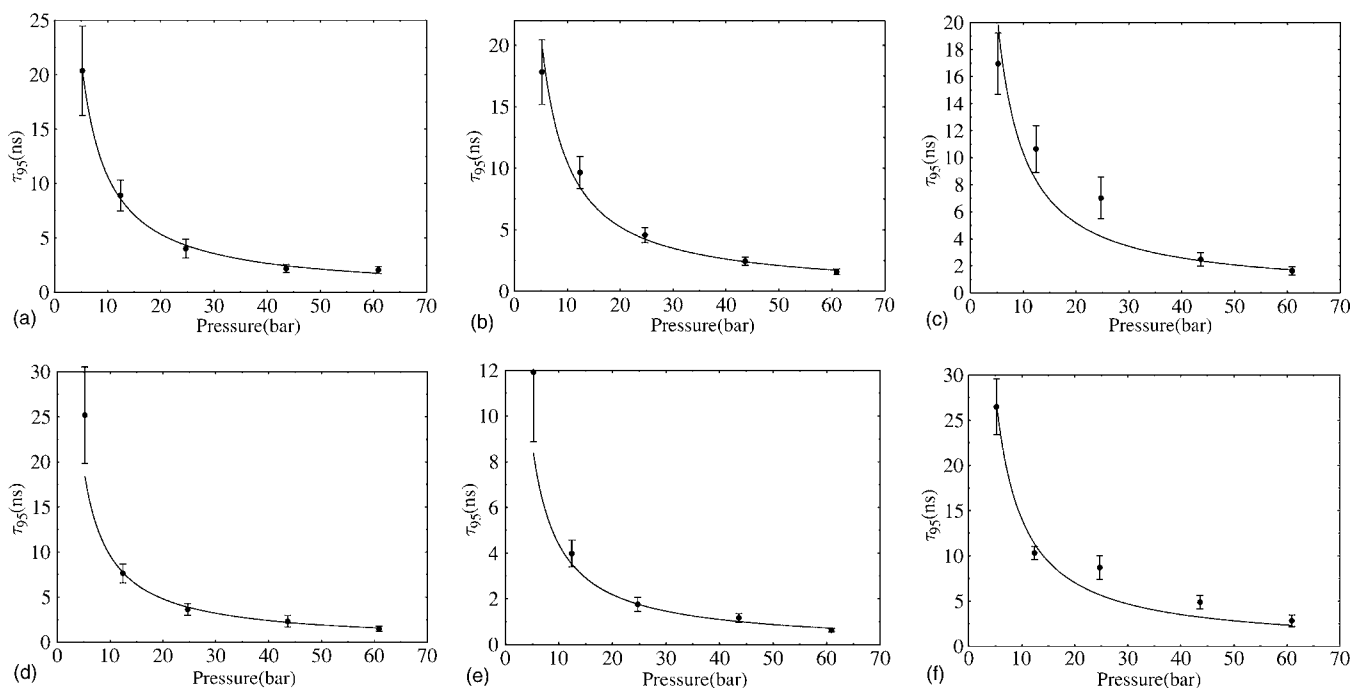
FIG. 4. τ_{95} as a function of the initial vapor pressure with different interaction models. Simulation data points are marked with circles, and the fitted function from Eq. (1) is plotted as solid lines. The simulated materials are the following: (a) EAM-Copper; (b) EAM-Silver; (c) RGL-Copper; (d) RGL-Silver; (e) EAM-Aluminum; (f) EAM-Platinum.

densation coefficient α_c, and the area of cluster in terms of diameter d_c, we can write Eq. (2) in the following form:

$$z_c = \frac{\pi d_c^2 \alpha_c (p_v - p_c)}{\sqrt{2\pi m k T_v}}, \qquad (3)$$

where z_c is the rate of coalescence of vapor atoms and p_c the loss in vapor pressure. In the current situation of condensation of strongly bound materials, the condensation coefficient α_c can be expected to be practically equal to 1, which is also observed in the simulations. We retain it in our calculations to enable generalization to other kinds of materials, but use $\alpha_c = 1$ in the evaluation. We can simplify our approach further by assuming that each added vapor atom increases the cluster volume by an equal characteristic amount V_u. By simple geometric arguments, this approximation gives the relation

TABLE I. Values for the constant C_c in Eq. (1) fitted to simulation results and calculated from the analytical model described in the text.

Potential model	C_c from fit to Eq. (1) (ns/bar)	C_c from Eq. (11) (ns/bar)
EAM Cu	107±9	74.37
RGL Cu	103±9	74.37
EAM Ag	105±7	75.74
RGL Ag	96±8	75.74
EAM Al	44±4	38.62
EAM Pt	141±8	110.8

$$\frac{d(d_c)}{dn_c} = \left(\frac{2V_u}{9\pi} \right)^{1/3} n_c^{-2/3}, \qquad (4)$$

where n_c is the number of atoms in the cluster. Furthermore, we can apply the ideal-gas law to the pressure terms in Eq. (3). Denoting the total number of vapor atoms in the system with n_{tot}, we can write the pressure loss p_c with the initial vapor pressure as follows:

$$p_c V_s = n_c k T_v, \quad p_v V_s = n_{tot} k T_v \Rightarrow p_c = p_v \frac{n_c}{n_{tot}}. \qquad (5)$$

V_s in Eq. (5) is the volume of the system in focus. The condensation rate z_c can be expressed as $\frac{dn_c}{dt}$. Combining Equations (3)–(5) gives us the following rate equation:

$$\frac{dn_c}{dt} = \sqrt{\frac{2}{\pi m_v k T_v}} \left(\frac{9\pi}{2V_u} \right)^{1/3} V_u \alpha_c p_v n_c^{2/3} \left(1 - \frac{n_c}{n_{tot}} \right). \qquad (6)$$

As discussed above, we observed very little evaporation in our simulations. The heat generated by condensation is mostly contained in intermediate clusters. The temperature of the vapor itself can be assumed to be the same as the temperature of the surrounding inert gas, which in our simulations was kept constant. If we consider Eq. (6), we see that most of the terms can be assumed constant in terms of n_c and t. We can rewrite the rate equation in a more practical shape by defining the constant

$$\lambda \equiv \sqrt{\frac{2}{\pi m_v k T_v}} \left(\frac{9\pi}{2V_u} \right)^{1/3} V_u \alpha_c, \qquad (7)$$

which gives us the expression

$$\lambda p_v dt = \frac{dn_c}{\left(1 - \dfrac{n_c}{n_{tot}}\right)n_c^{2/3}}. \tag{8}$$

Performing the variable change $u = n_c/n_{tot}$, $dn_c = n_{tot}du$, where u is the proportion of atoms in clusters over total number of atoms, and calculating the integral $t:0 \rightarrow \tau_s$, $u:n_0/n_{tot} \rightarrow s$ yield

$$\lambda p_v \tau_s = n_{tot}^{1/3} \int_{n_0/n_{tot}}^{s} \frac{du}{(1-u)u^{2/3}}, \tag{9}$$

where n_0/n_{tot} is the fraction of vapor atoms in the initial cluster. The integral on the right-hand side diverges at $s=1$. However, it still behaves reasonably smoothly around $s=0.95$. Moreover, it has no system dependent variables within, and therefore the value of the integral is the same for all materials studied. From now on, we will denote it as k_s, and Eq. (9) simplifies to

$$\tau_s = \frac{n_{tot}^{1/3}k_s}{\lambda p_v} = \frac{C_c}{p_v}, \tag{10}$$

where C_c corresponds to the constant used in our fitting procedure. Thus, our analytical model explains the $1/p_v$ behavior observed in the simulations for all materials.

Substituting Eq. (7) to Eq. (10) gives

$$C_c = \left(\frac{\sqrt{\pi}n_{tot}}{9\sqrt{2}}\right)^{1/3} \frac{\sqrt{kT_v}k_s}{\alpha_k} \frac{\sqrt{m_u}}{V_u^{2/3}}. \tag{11}$$

We evaluated C_c using a lower limit for the cluster size of $n_0 = 2$ atoms in the integral k_s and an atomic volume corresponding to that in an fcc crystal, $V_u = a^3/4$, where a is the equilibrium lattice constant. The values of C_c predicted from our model are compared with the fitted ones in Table I. The values are in very good agreement considering the approximations made in deriving the model. The about 20% discrepancy is most likely related to the cluster aggregation events.

The only terms characteristic to the material are the V_u and m_u. V_u is proportional to the cube of the lattice constant a. Thus, the characteristic dependence of C_c on material properties is

$$C_c \propto \frac{\sqrt{m_u}}{a^2}. \tag{12}$$

Plotting all the EAM metals to $\left(C_c, \frac{\sqrt{m_u}}{a^2}\right)$ coordinates shows us the distinct linear relation of Fig. 5. This gives additional credence to the derived model, since the part of the function that has no material dependent parameters acts the same way in all materials studied in this paper. This also gives us a tool to scale the condensation time or the resulting cluster size to different materials once the behavior of the modeled system is observed for some experimental vapor.

The dependencies obtained from our simulation model, namely, that the condensation time is proportional to inverse pressure and the predicted values of C_c, can be used to apply the current results to lower and variable pressures relevant in experimental inert gas condensation cluster-ion sources.
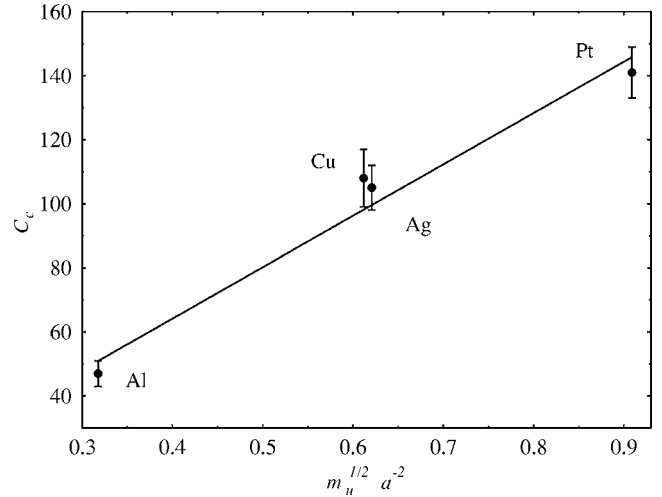
FIG. 5. Behavior of constant C_c used in fitting procedure compared to material dependent parameters in the derived model. Solid line is the linear fit through the values of C_c obtained from the simulations.

It is also possible to use the model to understand how a change in experimental conditions affects the cluster size. The condensation time can be estimated from flow of inert gas and chamber length and the initial metal vapor pressure by the rate of sputtering. To the authors' knowledge, there are no extensive experimental studies made on the time scale of cluster growth in the chamber of an inert gas condensation apparatus, especially in relation to different initial metal vapor pressures. Such a study could be analyzed based on the model derived in this paper. Existing results on cluster growth comparing different materials and initial metal vapor pressure give support to the model derived in this paper on a qualitative level. Cluster sizes resulting from different initial partial pressures of the condensing vapor are presented in Ref. 32. While the pressures used are far below what we used in our simulations, applied equal pressures of Zn and Mg vapors resulted in roughly 80% larger Mg clusters in diameter. Calculating from Eq. (12) yields a 42% smaller time constant C_c to Mg, which means that Mg reaching a certain cluster size takes 42% of the time needed to form the same size of cluster from Zn vapor. Since the time scales of growth are not known in the experiments, a direct comparison on the size is not possible. However, the prediction of our model of Mg clusters growing faster than Zn ones is at least in qualitative agreement with the experimental results.

IV. CONCLUSIONS

We calculated the time for a 1000 atom vapor to condensate into a single cluster at various vapor pressures for copper, silver, aluminum, and platinum by molecular dynamics simulation. We applied the thermostat only to the inert gas atoms to keep the simulated system as natural and realistic as possible. We ran ten simulations at each pressure for each material to get relatively good statistics for the behavior. The results were practically identical between the RGL and EAM potentials, which leads to the conclusion that the condensa-

tion rate is not sensitive to the interaction model used.

The pressure dependence of the condensation time appeared to obey the form $1/p$. We explained this by deriving a model from kinetic gas theory and using basic approximations of classical nucleation theory for a homogeneous vapor. The model can also quantitatively predict the growth speed for materials of different mass and lattice constant. The speed is lower for a larger mass and higher for a larger lattice constant.

[1] J. Aitken, Nature (London) **23**, 195 (1881).

[2] R. Becker and W. Döring, Ann. Chim. Phys. **30**, 232 (1935).

[3] J. Zeldovich, Zh. Eksp. Teor. Fiz. **12**, 525 (1942).

[4] J. Zeldovich, Acta Physicochim. URSS **18**, 1 (1943).

[5] W. Henkes, Z. Naturforsch. A **16**, 842 (1961).

[6] P. G. Bentley, Nature (London) **190**, 432 (1961).

[7] H. Vehkamäki, M. Dal Maso, T. Hussein, R. Flanagan, A. Hyvärinen, J. Lauros, J. Merikanto, P. Mönkkönen, M. Pihlatie, K. Salminen, L. Sogacheva, T. Thum, T. M. Ruuskanen, P. Keronen, P. P. Aalto, P. Hari, K. E. J. Lehtinen, Ü. Rannik, and M. Kulmala, Atmos. Chem. Phys. **4**, 2015 (2004).

[8] J. Raula, J. Shan, M. Nuopponen, A. Niskanen, H. Jiang, E. I. Kauppinen, and H. Tenhu, Langmuir **19**, 3499 (2003).

[9] C. J. Kelly, J. Fink, M. Brust, D. Bethell, and D. J. Schiffrin, Nature (London) **396**, 444 (1998).

[10] H. Haberland, M. Karrais, M. Mall, and Y. Thurner, J. Vac. Sci. Technol. A **10**, 3266 (1992).

[11] U. Kortshagen and U. Bhandarkar, Phys. Rev. E **60**, 887 (1999).

[12] H. Hahn and R. S. Averback, J. Appl. Phys. **67**, 1113 (1990).

[13] H. Haberland, M. Moseler, Y. Qiang, O. Rattunde, T. Reiners, and Y. Thurner, Surf. Rev. Lett. **3**, 887 (1996).

[14] H. Haberland, Z. Insepov, and M. Moseler, Phys. Rev. B **51**, 11061 (1995).

[15] I. Yamada, J. Matsuo, N. Toyoda, and A. Kirkpatrick, Mater. Sci. Eng., R. **34**, 231 (2001).

[16] R. E. Palmer, S. Pratontep, and H.-G. Boyen, Nat. Mater. **2**, 443 (2003).

[17] S. Thompson, J. Chem. Phys. **81**, 530 (1985).

[18] K. Yasuoka and M. Matsumoto, J. Chem. Phys. **109**, 8451 (1997).

[19] P. Krasnochtchekov, K. Albe, and R. S. Averback, Z. Metallkd. **94**, 1098 (2003).

[20] P. Krasnochtchekov and R. S. Averback, J. Chem. Phys. **122**, 044319 (2005).

[21] B. J. Alder and T. E. Wainwright, J. Chem. Phys. **27**, 1208 (1957).

[22] H. Berendsen, J. Postma, W. van Gunsteren, A. DiNola, and J. Haak, J. Chem. Phys. **81**, 3684 (1984).

[23] K. Nordlund, M. Ghaly, R. S. Averback, M. Caturla, T. Diaz de la Rubia, and J. Tarus, Phys. Rev. B **57**, 7556 (1998).

[24] K. Nordlund and R. S. Averback, Phys. Rev. B **59**, 20 (1999).

[25] S. M. Foiles, M. I. Baskes, and M. S. Daw, Phys. Rev. B **33**, 7983 (1986).

[26] V. Rosato, M. Guillopé, and B. Legrand, Philos. Mag. A **59**, 321 (1989).

[27] J. F. Ziegler, J. P. Biersack, and U. Littmark, *The Stopping and Range of Ions in Matter* (Pergamon, New York, 1985).

[28] C. Kittel, *Introduction to Solid State Physics*, 6th ed. (Wiley, New York, 1986).

[29] J. Westergre, H. Grönbeck, A. Rosen, and S. Nordholm, J. Chem. Phys. **109**, 9848 (1998).

[30] H. Vehkamäki, *Classical Nucleation Theory in Multicomponent Systems* (Springer, New York, 2006).

[31] W. C. Hinds, *Aerosol Technology: Properties, Behavior and Measurement of Airborne Particles* (Wiley, New York, 1999).

[32] C. G. Grandqvist and R. A. Buhrman, J. Appl. Phys. **47**, 2200 (1975).